BJR

Received: 4 August 2016 | Revised: 20 November 2016 | Accepted: 3 January 2017

https://doi.org/10.1259/bjr.20160662

Cite this article as:
Waduud MA, Sharaf A, Roy I, Lopez-Gonzalez R, Hart A, McGill D, et al. Validation of a semi-automated technique to accurately measure abdominal fat distribution using CT and MRI for clinical risk stratification. *Br J Radiol* 2017; **90**: 20160662.

FULL PAPER

Validation of a semi-automated technique to accurately measure abdominal fat distribution using CT and MRI for clinical risk stratification

[1]MOHAMMED A WADUUD, MB ChB, MSc, [1]AMAL SHARAF, MRCS, [1]IAIN ROY, MB ChB, [2]ROSARIO LOPEZ-GONZALEZ, PhD, [1,3]ANDREW HART, FRCS(Plast), PhD, [1]DAVID MCGILL, FRCS(Plast), MD, [2]GILES RODITI, FRCP, FRCR and [1,3]JOHN BIDDLESTONE, MRCS(Eng), PhD

[1]Canniesburn Plastic Surgery Unit, Glasgow Royal Infirmary, Glasgow, UK
[2]Department of Radiology, Glasgow Royal Infirmary, Glasgow, UK
[3]Centre for Cell Engineering, University of Glasgow, Glasgow, UK

Address correspondence to: Mr John Biddlestone
E-mail: *john.biddlestone@glasgow.ac.uk*

Objective: A valid method for accurate quantification of abdominal fat distribution (AFD) using both CT and MRI is described. This method will be primarily useful in the prospective risk stratification of patients undergoing reconstructive breast surgery. Secondary applications in many other clinical specialities are foreseen.
Methods: 15 sequential patients who had undergone breast reconstruction following both CT and MRI (30 scans) were retrospectively identified at our single centre. The AFD was quantified at the level of the L3 vertebra. Image analysis was performed by at least two independent operators using free software. Intra- and interobserver differences were assessed using Bland–Altman plots. Data were validated between imaging modalities by Pearson's correlation. Linear regression analyses were used to mathematically normalize results between imaging modalities.
Results: The method was statistically independent of rater bias (intra: Pearson's *R*—0.954–1.00; inter: 0.799–0.999). Strong relationships between imaging modalities were demonstrated and are independent of time between imaging (Pearson's *R* 0.625–0.903). Interchangeable mathematical models to normalize between imaging modality are shown.
Conclusion: The method described is highly reproducible and independent of rater bias. A strong interchangeable relationship exists between calculations of AFD on retrospective CT and MRI.
Advances in knowledge: This is the first technique to be applicable to scans that are not performed sequentially or in a research setting. Analysis is semi-automated and results can be compared directly, regardless of imaging modality or patient position. This method has clinical utility in prospective risk stratification and will be applicable to many clinical specialities.

INTRODUCTION

Obesity is a growing pandemic associated with many pathologies and resulting in significant morbidity and mortality.[1–6] Obesity is understood to have contributed to 3.4 million deaths worldwide in 2010.[7] The body mass index (BMI) is a widely used measure of obesity; however, when used alone, it is not useful in the diagnosis of obesity.[8] The accurate quantification of obesity is essential in studies investigating the outcomes as a function of obesity, so that trends may be reliably identified and interpreted. Alternative methods of measuring obesity include the quantification of total abdominal area (TAA), total abdominal fat (TAF), subcutaneous adipose tissue/extra-abdominal fat (EAF), abdominal visceral fat/intra-abdominal fat (IAF) and abdominal waist circumference (AWC), collectively known as the abdominal fat distribution (AFD). These important measurements are schematically represented in Figure 1. Measurement of the abdominal fat compartments is useful because the fat distribution is shown to be a more specific indicator of associated morbidity than BMI alone. For example, AWC and IAF have been shown to be more accurate measures of obesity than BMI.[9,10] In addition, there is a growing body of evidence highlighting the negative effects of IAF in comparison to EAF or peripheral fat.[11,12] IAF or central obesity is a particularly important predictor of morbidity since central obesity increases the direct exposure of visceral organs, such as the liver, to a high concentration of fatty acids and its metabolites resulting in additional metabolic and cardiovascular effects.[13,14]

Methods to measure AFD have been widely reported in both CT and MRI modalities.[15,16] CT imaging has the

Figure 1. Schematic of abdominal cross-section to display regions approximating to total abdominal area (TAA), total abdominal fat (TAF), subcutaneous adipose tissue/extra-abdominal fat (EAF), abdominal visceral fat/intra-abdominal fat (IAF) and abdominal waist circumference (AWC), collectively known as the abdominal fat distribution.

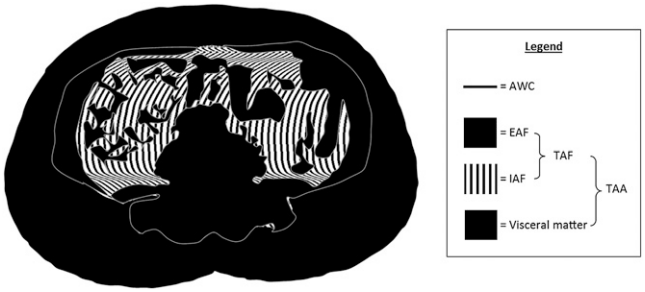

advantage of being relatively quick to acquire, with fewer contraindications and limitations than MRI. It also has the added advantage of being able to accurately and consistently quantify IAF.[17,18] CT imaging is limited because it exposes patients to a significant dose of radiation, which makes it difficult to clinically justify its use in certain patient groups. MRI is a reliable alternative as adipose tissue has a typical short longitudinal relaxation time compared with other tissues which makes the quantification of it possible. Measurements of AFD calculated from CT and MRI have been shown to have a strong positive correlation when performed according to pre-defined research criteria and in immediate succession.[19–24] However, no study has either validated or investigated the comparability of retrospective measurements of the AFD from CT and MRI performed solely due to clinical indication outside of pre-defined research/study criteria and undertaken at different points in time. Accurate quantification of AFD using existing, non-sequential CT or MRI is desirable because it is directly applicable to the current clinical environment and is predicted to provide valuable data when risk-assessing patients for elective surgery or interventions at no extra cost to the healthcare provider.

The primary aim of the study was to validate retrospective measurement of AFD on CT and MRI when performed without pre-defined research criteria and undertaken non-sequentially. The secondary aim was to determine the mathematical relationship between measurements of AFD across both imaging modalities. Achieving this secondary aim allows normalization of measurements between imaging modalities independent of scan timing and has great clinical utility. The ultimate aim of this study is to develop a method that allows measurement of AFD which can be performed by the clinician in the outpatient setting and used to stratify patients undergoing reconstructive breast surgery according to complications. These data would be practically used to guide reconstructive approach according to risk.

METHODS AND MATERIALS

This retrospective study was performed using anonymized CT and MRI from breast cancer patients prior to planned deep inferior epigastric perforator flap breast reconstruction at the Canniesburn Plastic Surgery Unit[25] (Glasgow, UK). Patients were identified from a prospectively maintained local database of all patients planned to undergo flap reconstruction at the department. This report is part of a larger study that aimed to identify relationships between complications of reconstructive breast surgery and specific measurements of AFD. The inclusion criteria for the larger study required it be limited to patients with carcinoma breast with reconstructive breast surgery. Patients were included if they had both pre-operative CT and MRI of the abdomen which could be downloaded from the national picture archiving communications system (Figure 2).[26] Pre-operative CT imaging was performed in the supine position with breath-hold to minimize motion artefact. MRI performed in the prone position because the acquisition time is greater than a breath-hold for MRI to get the required spatial resolution. Under these conditions, the prone position minimizes any movement of anterior abdominal wall and ensures that the region of interest is as close as possible to the coils. Flexible body array coils were used for all MRI. A transverse cross-section at the level of the third lumbar vertebra was used for image analysis. This technique had been previously demonstrated to be non-inferior to volumetric analysis of the adipose tissue of the abdomen and used in numerous previous studies.[20,26,27] Patients who had imaging at the appropriate level with portions missing or absent were excluded as analysis was likely to yield irreproducible and unreliable results.

Study approval

The study was approved by the local picture archiving communications system Clinical Advisory Group (C5507943), Caldicott Guardian and West of Scotland Research Ethics Service.

Image analysis and data collection

Demographic data collected included age, weight, height and BMI. Pre-operative abdominal CT and MR images were analysed for all patients who met the inclusion criteria. Eligibility for inclusion was determined by a single investigator. Transverse cross-sectional images were obtained at the level of the third lumber vertebra, which was identified by counting up from the sacrum on the sagittal view of the abdomen. Images were downloaded in the digital imaging and communications in medicine format, with preservation of the actual dimensions of

Figure 2. Flow chart illustrating the inclusion and exclusion of patients. CPSU, Canniesburn Plastic Surgery Unit (Glasgow, UK); DIEP, deep inferior epigastric artery perforator.

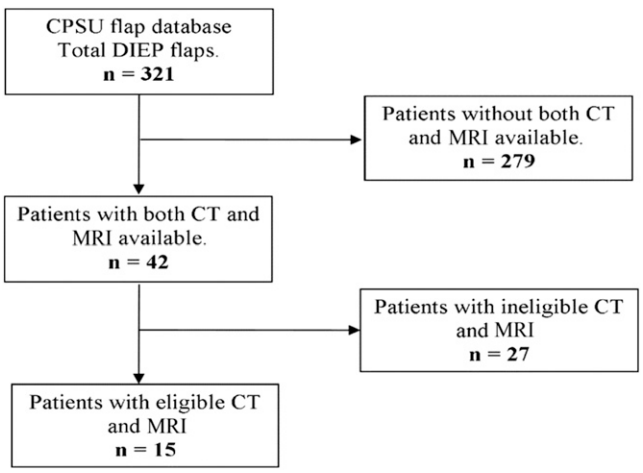

the patients to avoid magnification indices and scales, and anonymized prior to any analysis.[28] Each image was analysed by two individual investigators to identify any significant interobserver difference in measurements. All investigators analysing the images were blinded to the correlation of any image to either the respective case or the other imaging of the same case. The mean values were subsequently calculated using the values obtained by all investigators in order to ensure the most accurate value was used for comparative analysis. Images were also reanalysed by an individual investigator to identify any intraobserver differences in measurements.

All analysis was performed using the ImageJ software package (National Institute for Health, Bethesda, MD). A semi-automated threshold technique was used to remove investigator bias (Figure 3). This approach has the advantage of removing investigator bias and negates the requirement for hand-drawn regions of interest for fat evaluation that is both subjective and labour intensive. Using this technique, only manual muscle outlining is required. For all patients, measurements were made to quantify the TAA, TAF, EAF, IAF and AWC. Adipose tissue was differentiated from non-adipose tissue by setting modality-specific threshold values (Figure 3). CT images were analysed by setting the Hounsfield units between −190 and −30 to include maximal adipose tissue.[19,20,29] For MR images, the pulse sequence used was the true fast imaging with steady-state free precession. When using this sequence, the signal intensity is seen to be directly related to the T_2/T_1 ratio which is low for most solid tissues with the exception of fat and fluids. The true fast imaging with steady-state free precession sequence parameters were repetition

Figure 3. (a, b) Examples of transverse cross-section digital imaging and communications in medicine images downloaded from picture archiving communications system at the levels of the third lumbar vertebra using (a) CT and (b) MRI. (c) Illustration of the image analysis process for CT and MRI of two different patients. In brief, the abdominal waist circumference (AWC) and total abdominal area (TAA) were automatically calculated by the software package (Step 1). The threshold values were set by the user (Step 2) in order to identify and measure the total abdominal fat (TAF) (Step 3). The extra-abdominal fat (EAF) was calculated by excluding all intra-abdominal content (Step 4). Intra-abdominal fat was calculated by subtracting EAF from TAF.

A

B

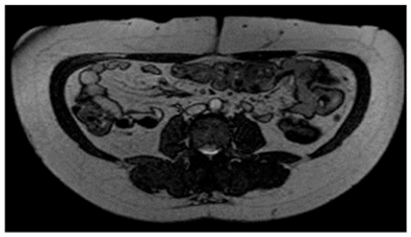

C

Process	Description	CT image analysis	MR image analysis
Step 1	Measurement of AWC (outline of shape) and TAA (shaded centrally).		
Step 2	Setting of threshold values.	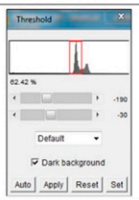	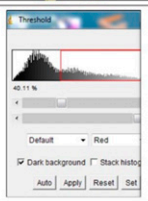
Step 3	Measurement of TAF (shaded).		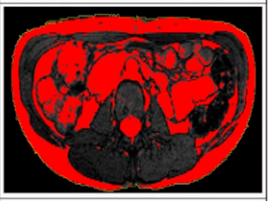
Step 4	Measurement of EAF (shaded).		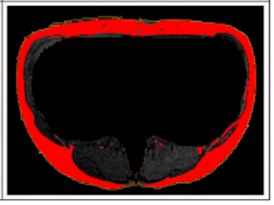

time = 4.01 ms, echo time = 1.71 ms, flip angle = 60°, matrix size = 256 × 176, field of view = 350 × 240 mm^2, slice thickness = 4 mm. We carried out a threshold segmentation technique by selecting the midpoint between the two peaks of the identified signal intensities in the histograms, with the presumption that mostly adipose tissue would be selected (Figure 3). Individual components of AFD were differentiated by defining boundaries. AWC was almost always highlighted automatically with the occasional image requiring hand-tracing. Abdominal muscles were hand-traced in all cases, so that the IAF area could be distinguished from the EAF area. All measurements were automatically calculated by the ImageJ software package (National Institutes of Health, Bethesda, MD: http://imagej.nih.gov/ij/).

Statistical analysis

All measurements were calculated as an area (cm^2) or length (cm). Continuous variables were reported as mean [standard deviation (SD), range] and compared using one-way analysis of variance with Holm–Sidak pairwise comparison. Inter- and intraobserver differences were evaluated by scatter plot with linear regression, with Pearson correlation and using Bland–Altman plots. For the Bland–Altman plots, the limits of agreement were calculated from the difference between the investigators' measurements for each fat compartment using the same imaging modality. To determine the mathematical relationship between imaging modalities, averaged measurements obtained for each parameter of AFD in both imaging modalities were plotted on a scatter graph so that linear regression analysis could be performed and Pearson's coefficient calculated. Regression formulas were used to describe the predictability of the findings of one imaging modality given the other. p-values <0.05 were considered statistically significant. Statistical significance denoted as: NS, $p > 0.05$; $^*p \leq 0.05$; $^{**}p \leq 0.01$; $^{***}p \leq 0.001$. Statistical analyses were performed using SigmaPlot® v. 12.0 (Systat Software Inc., San Jose, CA).[30]

RESULTS

In total, 15 patients had both CT and MR images that were suitable for comparative analysis (Figure 2). A total of 30 images were analysed. These images were performed between August 2009 and January 2015. MRI was typically performed at a later date than CT imaging with a mean time between scans of 68 days (77.8 SD, range 1–255 days). The average age of patients at the time of MRI was 48.7 years (±7.1 SD; range 31.7–57.7 years). 14 patients (93.3%) had data recorded relating height, weight and BMI; and all patients had measurements of AFD on CT and MRI (Table 1). No significant differences were identified in mean measurement of TAF, EAF and IAF between imaging modalities. By contrast, significant differences were demonstrated between mean TAA and AWC measurements (Table 1).

Validation of method

In order to determine the reliability of the measurement method, an assessment of intra- and interobserver variability was performed. A total of five measurements were made from each image, representing the parameters of AFD, resulting in a total of 150 measurements. Intraobserver variability was evaluated by comparing repeated measurements made by a single investigator. Interobserver variability was evaluated by comparing the measurements made by two independent investigators.

A formative assessment of intra- and interobserver variability was performed by scatter plot with linear regression, with

Table 1. Summary of patient demographic data and statistical comparison of measurements by imaging modality

Parameter	Value, mean ± standard deviation (range)	p-value[a]	Significance
Weight (kg)	67.5 ± 5.4 (59.0–77.9)		
Height (m)	1.65 ± 0.07 (1.55–1.79)		
BMI ($kg\,m^{-2}$)	24.9 ± 2.8 (20.5–32.4)		
Image analysis			
CT TAA (cm^2)	605.2 ± 76.5 (524.6–821.4)	<0.001	***
MRI TAA (cm^2)	513.1 ± 56.6 (433.3–629.0)		
CT TAF (cm^2)	298.4 ± 85.3 (178.1–505.7)	0.125	NS
MRI TAF (cm^2)	257.1 ± 54.5 (185.7–366.4)		
CT EAF (cm^2)	219.2 ± 62.5 (147.2–383.2)	0.091	NS
MRI EAF (cm^2)	184.2 ± 45.6 (117.4–273.7)		
CT IAF (cm^2)	79.2 ± 35.4 (28.2–165.6)	0.557	NS
MRI IAF (cm^2)	72.9 ± 21.1 (43.1–120.9)		
CT AWC (cm)	97.6 ± 6.6 (91.0–112.7)	0.03	*
MRI AWC (cm)	92.8 ± 5.0 (82.8–100.9)		

AWC, abdominal waist circumference; EAF, extra-abdominal fat; IAF, intra-abdominal fat; TAA, total abdominal area; TAF, total abdominal fat.
Statistical significance denoted as: $^*p \leq 0.05$; $^{**}p \leq 0.01$; $^{***}p \leq 0.001$; NS, $p > 0.05$.
[a]Following one-way analysis of variance with Holm–Sidak pairwise comparison.

Pearson's correlation and using Bland–Altman plots. For the Bland–Altman plots, the limits of agreement were calculated from the difference between the investigators' measurements for each fat compartment using the same imaging modality (Table 2 and Figure 4, and Supplementary Data). This approach confirmed that the intra- and interobserver discrepancies were not statistically significant (Table 2 and Figure 4, and Supplementary Data). This finding is important because it validates the method of measurement across imaging modalities, performed without pre-defined research criteria and undertaken non-sequentially in keeping with the primary aim of this study.

Mathematical normalization between imaging modalities

To achieve normalization between the imaging modalities, measurements of AFD were plotted on scatter graphs (Figure 5). Regression analyses highlighted highly significant positive correlations between all measurements of AFD obtained from CT and MRI (Table 3). The correlation for AWC was notably lower than all other parameters of AFD but remained statistically significant. Pearson's correlation coefficient calculations were performed to mathematically describe the trends observed (Table 3 and Figure 5). As all correlation was statistically significant, regression lines and their formulae were calculated for TAA, TAF, EAF, IAF and AWC (Figure 5). The formulae calculated facilitated the conversion of values obtained from MR image analysis to equivocal CT image analysis values. Therefore, when the MR measurements were known, the equivocal CT measurements could be calculated using the following formulae: CT TAA = 18.410 + (1.144 × MR TAA), CT TAF = −65.485 + (1.416 × MR TAF), CT EAF = 6.166 + (1.157 × MR EAF), CT IAF = −27.938 + (1.470 × MR IAF) and CT AWC = 20.861 + (0.828 × MR AWC).

DISCUSSION

A number of studies have reported the reliability of prospective measurements of AFD using CT and MRI, comparing a range of methods and technical settings.[19–24] This is the first study to demonstrate a strong statistically significant relationship between retrospective measurements of AFD on CT and MRI. The scans used in this study were not performed sequentially or in a research setting and as such faithfully represent the current clinical environment. We demonstrate a robust and reproducible

Table 2. Summary of intra- and interobserver variability in measurements of abdominal fat distribution by imaging modality

Parameter	Intraobserver variability				Interobserver variability			
	Bias	Limit lower	Limit upper	Pearson's *R*	Bias	Limit lower	Limit upper	Pearson's *R*
CT TAA	611.08 ± 75.28 (538.67–823.65)				605.20 ± 76.54 (524.6–821.4)			
	−0.02	−4.05	4.01	1.00***	−11.77	−30.88	7.32	0.992***
CT TAF	301.05 ± 85.04 (182.92–507.73)				298.39 ± 85.34 (178.14–505.66)			
	−0.21	−1.59	1.18	1.00***	−5.53	−13.06	2.00	0.999***
CT EAF	222.04 ± 62.15 (151.36–385.56)				219.19 ± 62.47 (147.23–383.19)			
	−0.071	−4.11	2.69	1.00***	−6.42	−13.40	0.55	0.998***
CT IAF	79.01 ± 35.72 (27.90–166.10)				79.20 ± 35.44 (28.24–165.64)			
	0.51	−2.12	3.13	0.999***	0.89	−2.56	4.35	0.999***
CT AWC	97.54 ± 6.53 (90.97–112.65)				97.62 ± 6.59 (91.00–112.70)			
	0.07	−1.34	1.48	0.995***	0.24	−1.63	2.10	0.992***
MRI TAA	512.84 ± 56.35 (433.36–629.11)				513.11 ± 56.63 (433.25–628.99)			
	−1.17	−7.18	4.85	0.999***	−0.64	−11.44	10.16	0.995***
MRI TAF	264.06 ± 54.91 (193.17–364.68)				257.05 ± 54.45 (185.70–366.40)			
	2.42	−5.55	10.39	0.998***	−11.60	−50.21	27.02	0.937***
MRI EAF	186.74 ± 45.96 (123.20–274.47)				184.18 ± 45.64 (117.43–273.67)			
	0.92	−6.01	7.86	0.998***	−4.20	−18.32	9.92	0.988***
MRI IAF	77.32 ± 23.24 (46.46–130.09)				72.87 ± 21.10 (43.10–120.88)			
	1.49	−5.40	8.39	0.989***	−7.40	−32.90	18.11	0.831***
MRI AWC	93.14 ± 5.00 (82.72–103.04)				92.75 ± 4.98 (82.76–100.86)			
	−0.66	−3.81	2.48	0.954***	−1.45	−7.98	5.09	0.799***

AWC, abdominal waist circumference; EAF, extra-abdominal fat; IAF, intra-abdominal fat; TAA, total abdominal area; TAF, total abdominal fat.
Bias, limits and Pearson correlation coefficients relate to graphs in Figure 4 and Supplementary Data.
Statistical significance is denoted as: NS $p > 0.05$; *$p \leq 0.05$; **$p \leq 0.01$; ***$p \leq 0.001$.

Figure 4. (a) Determination of intra-observer variability: representative scatter plots to compare repeated single rater measurements with regression line (solid line) and 95% confidence intervals (dotted lines) are presented alongside Bland-Altman graphs to demonstrate variability of measurements about the mean (central line) and 95% confidence intervals (upper and lower blue lines). (b) Determination of inter-observer variability: similar representative scatter plots and Bland Altman graphs are shown to those in (a). In both examples, data for TAF are shown. For plots of each parameter see Supplementary Data. A summary of bias and limits are shown in Table 2.

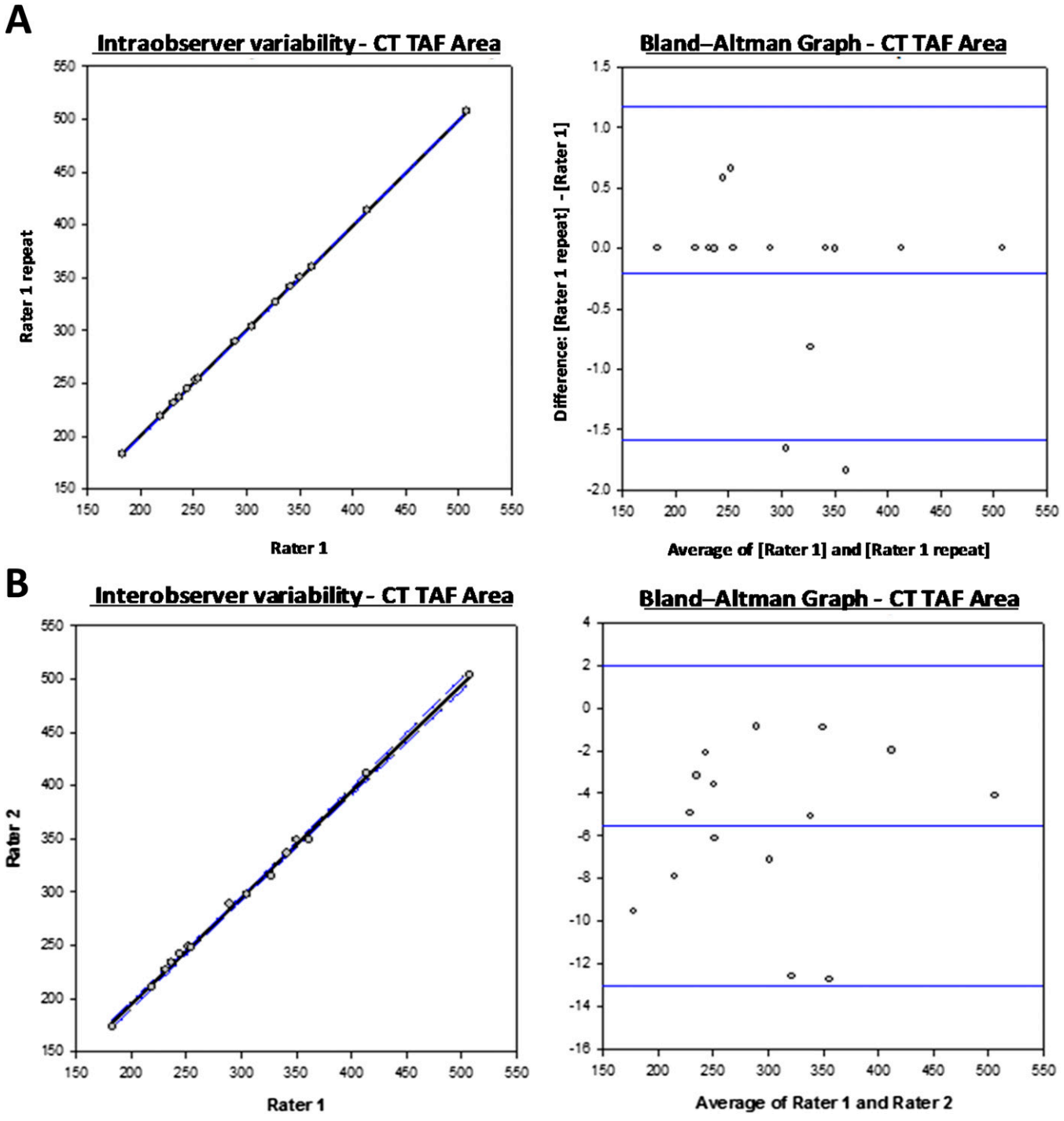

method to compare measurements of AFD from retrospective imaging performed solely on clinical merit at different points in time. Similar to previous prospective studies, strong positive linear correlations have been identified and mathematical equations developed to normalize measurements between imaging modalities, for TAA, TAF, EAF, IAF and AWC are described.

Measurements of EAF and IAF using both CT and MRI were first compared by Ross et al[24] in a cohort of 17 rats who, unlike our study cohort, were all subjected to total body imaging. With both modalities, imaging was performed with the rats in the supine position, slices taken at identical positions and imaging was performed in immediate succession. They reported no

Figure 5. Scatter graphs of measurements obtained with MRI and CT imaging for (a) total abdominal area (TAA), (b) total abdominal fat (TAF), (c) extra-abdominal fat (EAF), (d) intra-abdominal fat (IAF) and (e) abdominal waist circumference (AWC). All coefficients represent statistically significant positive correlations (Table 3). The regression lines are shown (solid line). *R*, Pearson's correlation coefficient. Statistical significance denoted as: $*p \leq 0.05$; $**p \leq 0.01$; $***p \leq 0.001$; NS, $p > 0.05$.

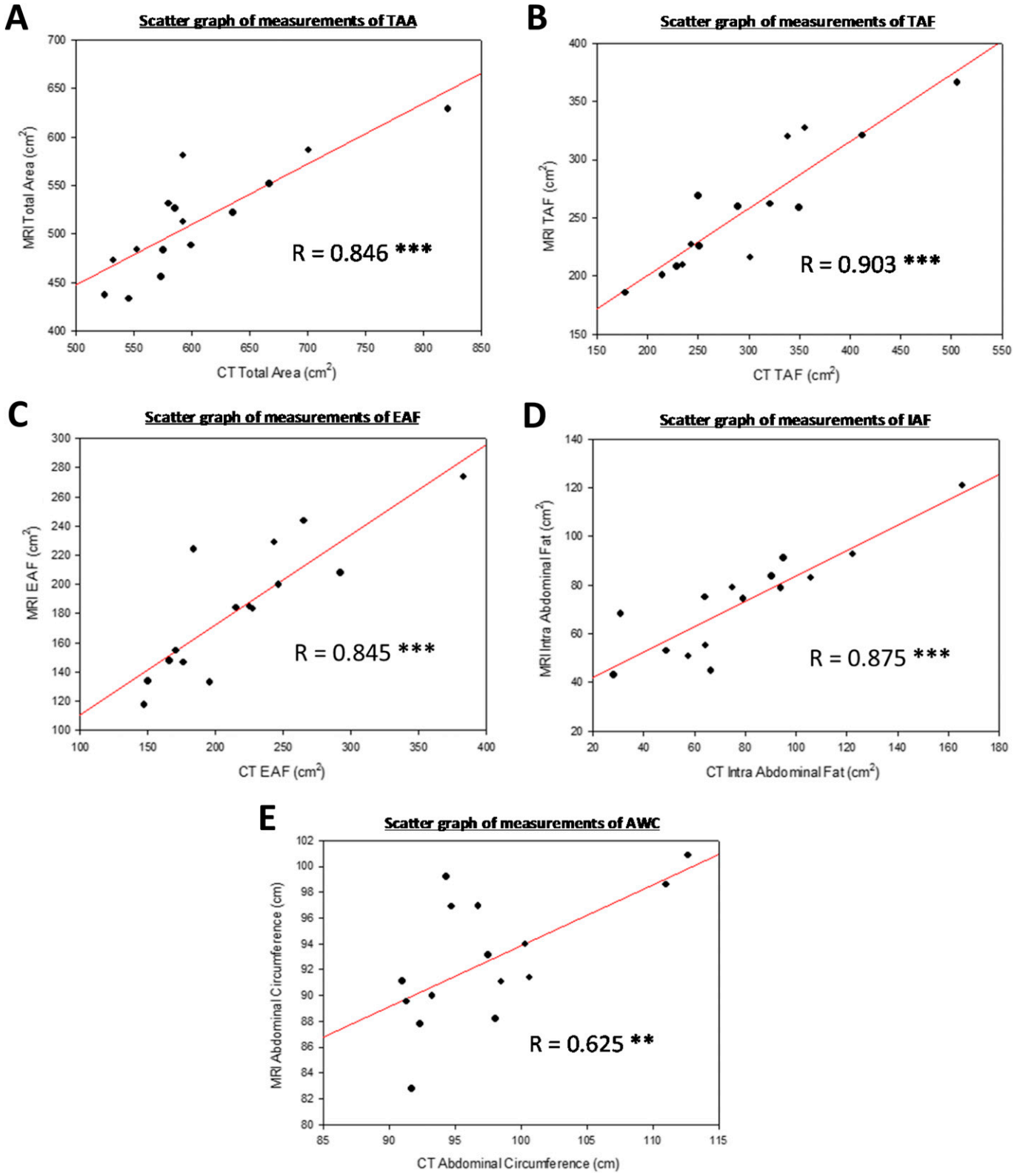

Table 3. Comparative analysis of CT and MRI measurements using Pearson's product moment correlation

Comparison	Pearson's correlation		Significance
	R	*p*-value	
CT TAA (cm^2) *vs* MRI TAA (cm^2)	0.846	<0.001	***
CT TAF (cm^2) *vs* MRI TAF (cm^2)	0.903	<0.001	***
CT EAF (cm^2) *vs* MRI EAF (cm^2)	0.845	<0.001	***
CT IAF (cm^2) *vs* MRI IAF (cm^2)	0.875	<0.001	***
CT AWC (cm) *vs* MRI AWC (cm)	0.625	0.01	**

AWC, abdominal waist circumference; EAF, extra-abdominal fat; IAF, intra-abdominal fat; *R*, correlation coefficient; TAA, total abdominal area; TAF, total abdominal fat.
Statistical significance denoted as: *$p \leq 0.05$; **$p \leq 0.01$; ***$p \leq 0.001$; NS, $p > 0.05$.

significant differences in measurements of IAF between the two modalities, and identified strong positive correlations when comparing measurements of EAF and IAF. In keeping with our own findings, they noted statistically significant differences when comparing mean measurements of TAF and EAF between modalities. The first human comparative study was reported by Seidell et al.[20] This prospective study subjected seven healthy male volunteers to successive CT and MRI. Similar to the study by Ross et al, imaging was performed with the subjects in the supine position; however, in this study a single slice transverse image was analysed taken midway between the lower rib margins and iliac crests. Seidell et al reported strong correlations across modalities when measuring TAF, EAF and IAF. These prospective findings have since been confirmed by a more recent study by Klopfenstein et al[19] where successive CT and MRI were performed on 27 patients. In our study, imaging was performed in a non-sequential manner. We recognize the small participant numbers are a limitation of this study. Despite this, we found that measurements of TAF, EAF and IAF all appear to be independent of imaging modality or timing of imaging.

As highlighted above and in contrast to previous studies, the images used in our analyses were undertaken at different time points. The time between imaging studies did not appear to alter previously observed positive correlations when measuring AFD on CT and MRI. This suggests imaging performed up to a year apart could be reliably analysed and compared as demonstrated in our cohort. The reliability of this analysis could be potentially confounded by significant weight loss or gain that was not observed in our cohort. A further advantage of this approach is its independence of patient position. All of the prospective studies intentionally positioned patients in the supine position when obtaining images with both modalities. However, this was not possible in our retrospective cohort of patients, as CT imaging analysed was performed in the supine position and MRI performed in the prone position because the acquisition time is greater than a breath-hold for MRI to get the required spatial resolution. We hypothesize that this may have contributed to the significant difference noted in mean TAA and AWC measurements. Despite this, strong relationships were still demonstrated between TAA and AWC measurements collectively. Patient positioning may also partly explain why MR measurements of TAA and AWC were consistently lower than their counterpart CT measurements, as fat in the anterior abdomen may have been compressed over the longitudinal plane when prone in a way that is restricted by the thicker skin and visceral support when supine. By contrast, the TAF, EAF and IAF appear to be less affected by patient position and extrinsic compression. Since EAF and IAF combine to form TAF, it is unsurprising that these measurements are collectively unchanged by imaging modality.

In our analysis of CT images, we used Hounsfield units alone to estimate AFD. This technique is in contrast to Potretzke et al,[31] who highlighted that CT image analysis using this method alone to identify adipose tissue could lead to overestimation of AFD due to the incorrect inclusion of colonic content. They recommended the exclusion of such artefact using specialist software and use of individualized Hounsfield cut-off values to improve correlation of measurements between CT and MRI. Potretzke et al did, however, note that the use of individually determined cut-off values was positively correlated with significant interobserver differences. We decided to adopt a homogeneous protocol for CT image analysis with the aim to minimize inter- and intraobserver differences and reduce time-wastage. In keeping with this, a greater percentage of interobserver differences were noted on MR image analyses in which individually determined threshold segmentation was required.

Finally, we also considered the use of a volume-based *vs* single slice technique for assessment of AFD across imaging modalities. Borkan et al[27] demonstrated that when measuring AFD, there was no additional advantage of volumetric analysis from imaging performed at multiple levels. We therefore decided to adopt the single-slice technique at the level of the third lumbar vertebra, as this had also been previously utilized in numerous previous studies.[19,20,22]

CONCLUSION

These data show that the measurements of AFD taken from CT and MR images are valid for our patient population since intra- and interobserver differences are not significant regardless of imaging modality. In addition, a strong interchangeable relationship was demonstrated between retrospective measurements of TAA, TAF, EAF, IAF and AWC on MRI and CT imaging performed without pre-defined research criteria and undertaken non-sequentially. The timing of imaging and positioning of the patient did not affect the linear relationship of AFD

measurements on both imaging modalities. Based on our data, a new method for normalization of measurements between imaging modalities independent of scan timing is demonstrated, with results comparable to previously published prospective studies.

The methodology of this study has been designed to allow its findings to be utilized by a medical researcher in any speciality wishing to investigate outcomes as a function of AFD. The ultimate aim of this study was to develop a method that allows measurement of AFD which can be performed by the clinician in the outpatient setting and used to stratify patients undergoing reconstructive breast surgery according to complications. These data would be practically used to guide reconstructive approach according to risk but are foreseeably useful in the risk stratification of a range of procedures performed across several surgical specialities.

A system whereby valid measurements can be easily made from retrospective images has been described that provides an opportunity for researchers and clinicians to determine AFD without additional cost. It is hoped that the cost effectiveness and normalization features of this method will facilitate its inclusion in larger study populations as both CT and MRI may be reliably and interchangeably used.

CONFLICTS OF INTEREST

None declared.

FUNDING

JB is a Scottish Clinical Research Excellence Development Scheme Clinical Lecturer funded by the National Health Service Education for Scotland at the University of Glasgow, Scotland, UK. No external funding sources were required to conduct this work.

REFERENCES

1. Cole TJ, Bellizzi MC, Flegal KM, Dietz WH. Establishing a standard definition for child overweight and obesity worldwide: international survey. *BMJ* 2000; **320**: 1240. doi: https://doi.org/10.1136/bmj.320.7244.1240
2. Finucane MM, Stevens GA, Cowan MJ, Danaei G, Lin JK, Paciorek CJ, et al. National, regional, and global trends in body-mass index since 1980: systematic analysis of health examination surveys and epidemiological studies with 960 country-years and 9.1 million participants. *Lancet* 2011; **377**: 557–67. doi: https://doi.org/10.1016/S0140-6736(10)62037-5
3. Flegal KM, Carroll MD, Ogden CL, Curtin LR. Prevalence and trends in obesity among US adults, 1999–2008. *JAMA* 2010; **303**: 235–41. doi: https://doi.org/10.1001/jama.2009.2014
4. Malik VS, Willett WC, Hu FB. Global obesity: trends, risk factors and policy implications. *Nat Rev Endocrinol* 2013; **9**: 13–27. doi: https://doi.org/10.1038/nrendo.2012.199
5. Must A, Strauss RS. Risks and consequences of childhood and adolescent obesity. *Int J Obes Relat Metab Disord* 1999; **23**(Suppl. 2): S2–11. doi: https://doi.org/10.1038/sj.ijo.0800852
6. Wilson PW, D'Agostino RB, Sullivan L, Parise H, Kannel WB. Overweight and obesity as determinants of cardiovascular risk: the Framingham experience. *Arch Intern Med* 2002; **162**: 1867–72. doi: https://doi.org/10.1001/archinte.162.16.1867
7. Lim SS, Vos T, Flaxman AD, Danaei G, Shibuya K, Adair-Rohani H, et al. A comparative risk assessment of burden of disease and injury attributable to 67 risk factors and risk factor clusters in 21 regions, 1990–2010: a systematic analysis for the Global Burden of Disease Study 2010. *Lancet* 2013; **380**: 2224–60. doi: https://doi.org/10.1016/S0140-6736(12)61766-8
8. Romero-Corral A, Somers VK, Sierra-Johnson J, Thomas RJ, Collazo-Clavell M, Korinek J, et al. Accuracy of body mass index in diagnosing obesity in the adult general population. *Int J Obes (Lond)* 2008; **32**: 959–66. doi: https://doi.org/10.1038/ijo.2008.11
9. Burkhauser RV, Cawley J. Beyond BMI: the value of more accurate measures of fatness and obesity in social science research. *J Health Econ* 2008; **27**: 519–29. doi: https://doi.org/10.1016/j.jhealeco.2007.05.005
10. Savva S, Tornaritis M, Savva M, Kourides Y, Panagi A, Silikiotou N, et al. Waist circumference and waist-to-height ratio are better predictors of cardiovascular disease risk factors in children than body mass index. *Int J Obes* 2000; **24**: 1453–8. doi: https://doi.org/10.1038/sj.ijo.0801401
11. Taksali SE, Caprio S, Dziura J, Dufour S, Calí AM, Goodman TR, et al. High visceral and low abdominal subcutaneous fat stores in the obese adolescent: a determinant of an adverse metabolic phenotype. *Diabetes* 2008; **57**: 367–71. doi: https://doi.org/10.2337/db07-0932
12. Nakamura T, Tokunaga K, Shimomura I, Nishida M, Yoshida S, Kotani K, et al. Contribution of visceral fat accumulation to the development of coronary artery disease in non-obese men. *Atherosclerosis* 1994; **107**: 239–46. doi: https://doi.org/10.1016/0021-9150(94)90025-6
13. Warren M, Schreiner PJ, Terry JG. The relation between visceral fat measurement and torso level—is one level better than another? The Atherosclerosis Risk in Communities Study, 1990–1992. *Am J Epidemiol* 2006; **163**: 352–8. doi: https://doi.org/10.1093/aje/kwj049
14. Pischon T, Boeing H, Hoffmann K, Bergmann M, Schulze M, Overvad K, et al. General and abdominal adiposity and risk of death in Europe. *N Engl J Med* 2008; **359**: 2105–20. doi: https://doi.org/10.1056/NEJMoa0801891
15. Shuman WP, Morris LL, Leonetti DL, Wahl PW, Moceri VM, Moss AA, et al. Abnormal body fat distribution detected by computed tomography in diabetic men. *Invest Radiol* 1986; **21**: 483–7. doi: https://doi.org/10.1097/00004424-198606000-00007
16. Staten M, Totty W, Kohrt W. Measurement of fat distribution by magnetic resonance imaging. *Invest Radiol* 1989; **24**: 345–9. doi: https://doi.org/10.1097/00004424-198905000-00002
17. Kvist H, Chowdhury B, Sjöström L, Tylen U, Cederblad A. Adipose tissue volume determination in males by computed tomography and 40K. *Int J Obes* 1988; **12**: 249–66.
18. Kvist H, Chowdhury B, Grangård U, Tylen U, Sjöström L. Total and visceral adipose-tissue volumes derived from measurements with computed tomography in adult men and women: predictive equations. *Am J Clin Nutr* 1988; **48**: 1351–61.
19. Klopfenstein B, Kim M, Krisky C, Szumowski J, Rooney W, Purnell J. Comparison of 3 T MRI and CT for the measurement of visceral and subcutaneous adipose tissue in humans.

Br J Radiol 2012; **85**: e826. doi: https://doi.org/10.1259/bjr/57987644

20. Seidell JC, Bakker C, van der Kooy K. Imaging techniques for measuring adipose-tissue distribution—a comparison between computed tomography and 1.5-T magnetic resonance. *Am J Clin Nutr* 1990; **51**: 953–7.
21. Gomi T, Kawawa Y, Nagamoto M, Terada H, Kohda E. Measurement of visceral fat/subcutaneous fat ratio by 0.3 Tesla MRI. *Radiat Med* 2005; **23**: 584–7.
22. Kullberg J, Brandberg J, Angelhed J, Frimmel H, Bergelin E, Strid L, et al. Whole-body adipose tissue analysis: comparison of MRI, CT and dual energy X-ray absorptiometry. *Br J Radiol* 2009; **82**: 123–30.
23. Ohsuzu F, Kosuda S, Takayama E, Yanagida S, Nomi M, Kasamatsu H, et al. Imaging techniques for measuring adipose-tissue distribution in the abdomen: a comparison between computed tomography and 1.5-Tesla magnetic resonance spin-echo imaging. *Radiat Med* 1997; **16**: 99–107.
24. Ross R, Leger L, Guardo R, De Guise J, Pike BG. Adipose tissue volume measured by magnetic resonance imaging and computerized tomography in rats. *J Appl Physiol* 1991; **70**: 2164–72.
25. Canniesburn Plastic Surgery Unit. Canniesburn Plastic Surgery Unit Online; 2015 [Cited 25 February 2016]. Available from: https://www.canniesburn.org/home/4590179330
26. Cooke RE Jr, Gaeta MG, Kaufman DM, Henrici JG. Picture archiving and communication system. *Google Patents* 2003.
27. Borkan GA, Gerzof SG, Robbins AH, Hults D, Silbert C, Silbert J. Assessment of abdominal fat content by computed tomography. *Am J Clin Nutr* 1982; **36**: 172–7.
28. Pianykh OS. *Digital imaging and communications in medicine (DICOM): a practical introduction and survival guide*. Berlin, Germany: Springer Science & Business Media; 2009.
29. Nemoto M, Yeernuer T, Masutani Y, Nomura Y, Hanaoka S, Miki S, et al. Development of automatic visceral fat volume calculation software for CT volume data. *J Obes* 2014; **2014**: 495084. doi: https://doi.org/10.1155/2014/495084
30. Scientific J. *SigmaPlot scientific graphing software—user's manual*. San Rafael, CA: Jandel Scientific; 1986.
31. Potretzke AM, Schmitz KH, Jensen MD. Preventing overestimation of pixels in computed tomography assessment of visceral fat. *Obes Res* 2004; **12**: 1698–701. doi: https://doi.org/10.1038/oby.2004.210